

**MORPHOMETRY, VOTES-ANALYSIS AND CALIBRATION IMPROVEMENTS OF CRATER DETECTION ALGORITHMS BASED ON EDGE DETECTORS AND RADON/HOUGH TRANSFORM.**  
 G. Salamunićcar<sup>1,2</sup> and S. Lončarić<sup>2</sup>, <sup>1</sup>AVL-AST d.o.o., Av. Dubrovnik 10/II, HR-10020 Zagreb-Novi Zagreb, Croatia, gsc@ieee.org, <sup>2</sup>Faculty of Electrical Engineering and Computing, University of Zagreb, Unska 3, HR-10000 Zagreb, Croatia, sven.loncaric@fer.hr.

**Summary:** Six previously implemented Crater Detection Algorithms (CDAs) were improved using morphometry measurements (some new and some improved), votes-analysis and calibration. The results were analyzed using the Framework for Evaluation of CDAs (FECDA).

**Introduction:** CDAs' applications range from dating planetary surfaces [1] to advanced statistical analysis [2]. CDAs are an important subject of recent scientific research [3-10]. Additional overview of CDA-related literature is given in [11]. In our previous work on CDAs, we proposed: (1) implementation based on standard gradient edge detectors and Radon/Hough transform [12-13]; and (2) several CDAs' specific improvements of the initial implementation [14-15].

**Methods:** The new methods and the improvements of the methods from previous work [15] are as follows.

*New morphometry measurements.* Automated measurements of crater rim and central peak are performed using 2-D crater profile. Associate volumes (profile surfaces) are compared to the volume of a crater itself. The circular consistency [14] of these features is additionally measured. The experiments show that the higher volumes and circularity mean the higher probability that detected feature is a crater.

*Improved morphometry measurements.* An automated detection of radial range where a crater is preserved is performed. The purpose is to check the circular consistency [14] only on the preserved part of a crater. In combination with the appropriate weight factor which depends on radial range, this increases overall performance. In order to improve tuning [14], additionally is performed: (1) an automated detection of

smaller circular features inside a larger one; (2) an automated depth/diameter measurement; (3) usage of more combinations and previously computed values.

*Circularity analysis of parameter space.* This new method evaluates parameter space in the same way as the circularity consistency evaluates 3-D crater shape [14]. The experiments show that the circularity of votes in parameter space is higher at craters' centers than in the centers of false detections. Therefore, this new measurement is used to improve overall performance.

*Calibration of resulting catalogue.* This new method multiplies probability that the detected feature is a crater with calibration factor. This factor depends only on a detected radius and increases with the increase of a radius. This partially compensates differences in morphology between small and large craters.

*Other changes.* The radius range is increased from 5~10 to 5~28 pixels while the optimal gradient is the same as in the previous work [15]. Numerous other parameters are also optimized.

**Results:** The obtained results are shown in Table 1. The analysis using F-ROC and detected edges are shown in Fig. 1. For evaluation of the results, from FECDA [11] the following were used: (1) 1/64° MOLA data; (2) the older GT-17582 catalogue [11] (and not the newer GT-57633 catalogue [16]) so that the results can be compared with the previous work [15]; and (3) Topolyzer application.

**Conclusion:** As the results show, CDAs were significantly improved using morphometry measurements, votes-analysis and calibration. Only ~3.24% of the craters from the GT-17582 catalogue are still undetected, mostly highly eroded (ghost) craters.

**Table 1:** Used gradient edge detectors and obtained results before and after modifications described in this paper.

operator	1. Pixel-Difference	2. Separated-Pixel-Difference	3. Roberts	4. Prewitt	5. Sobel	6. Frei-Chen
<b>before:</b>						
<i>TPs</i>	16447	16489	16434	16451	16471	16463
<i>AUROC<sub>1τ</sub></i>	78.774%	79.993%	78.225%	79.648%	79.784%	79.693%
<i>AUROC<sub>2τ</sub></i>	83.652%	84.644%	83.298%	84.162%	84.332%	84.216%
<i>AUROC<sub>5τ</sub></i>	88.111%	88.765%	87.866%	88.377%	88.529%	88.444%
<b>after:</b>						
<i>TPs</i>	16975	17013	16963	17008	17005	17000
<i>AUROC<sub>1τ</sub></i>	86.243%	86.975%	85.733%	86.826%	86.833%	86.829%
<i>AUROC<sub>2τ</sub></i>	89.841%	90.492%	89.517%	90.338%	90.352%	90.345%
<i>AUROC<sub>5τ</sub></i>	92.990%	93.483%	92.764%	93.316%	93.372%	93.325%

**Acknowledgements:** To colleagues D. Gržanić, M. Karas, D. Katušić, S. Katušić, J. Lucić, D. Mehić, V. Primorac, B. Spasić, Lj. Šare and D. Zorić for providing computers for the cluster which was used for faster computation of optimal parameters for CDAs.

**References:** [1] Hartmann W. K. and Neukum G. (2001) *Space Sci. Reviews*, 96, 165-194. [2] Salamunićcar G. (2004) *Adv. Space Res.*, 33, 2281-2287. [3] Michael G. G. (2003) *Planet. and Space Sci.*, 51, 563-568. [4] Cooper G. R. J. and Cowan D. R. (2004) *Comp. & Geosci.*, 30, 101-105. [5] Kim J. R. et al. (2005) *PERS*, 71, 1205-1217. [6] Sawabe Y. et al. (2006) *Adv. Space Res.*, 37, 21-27. [7] Bue B. D. and Stepinski T. F. (2007) *IEEE Trans. on Geosci. and*

*Remote Sensing*, 45, 265-274. [8] Bandeira L. et al. (2007) *IEEE Trans. on Geosci. and Remote Sensing*, 45, 4008-4015. [9] Krøgli S. O. et al. (2007) *Norwegian Journal of Geology*, 87, 157-166. [10] Martins R. et al. (in press), *IEEE Geosci. and Rem. Sensing Lett.*, doi:10.1109/LGRS.2008.2006004. [11] Salamunićcar G. and Lončarić S. (2008) *Adv. Space Res.*, 42, 6-19. [12] Novosel H. et al. (2007) *LPS XXXVIII*, Abstract #1351. [13] Knežević H. et al. (2008) *LPS XXXIX*, Abstract #1378. [14] Salamunićcar G. and Lončarić S. (2007) *7<sup>th</sup> Int. Conf. on Mars*, Abstract #3066. [15] Salamunićcar G. and Lončarić S. (2008) *LPS XXXIX*, Abstract #1375. [16] Salamunićcar G. and Lončarić S. (2008) *Planet. and Space Sci.*, 56, 1992-2008.

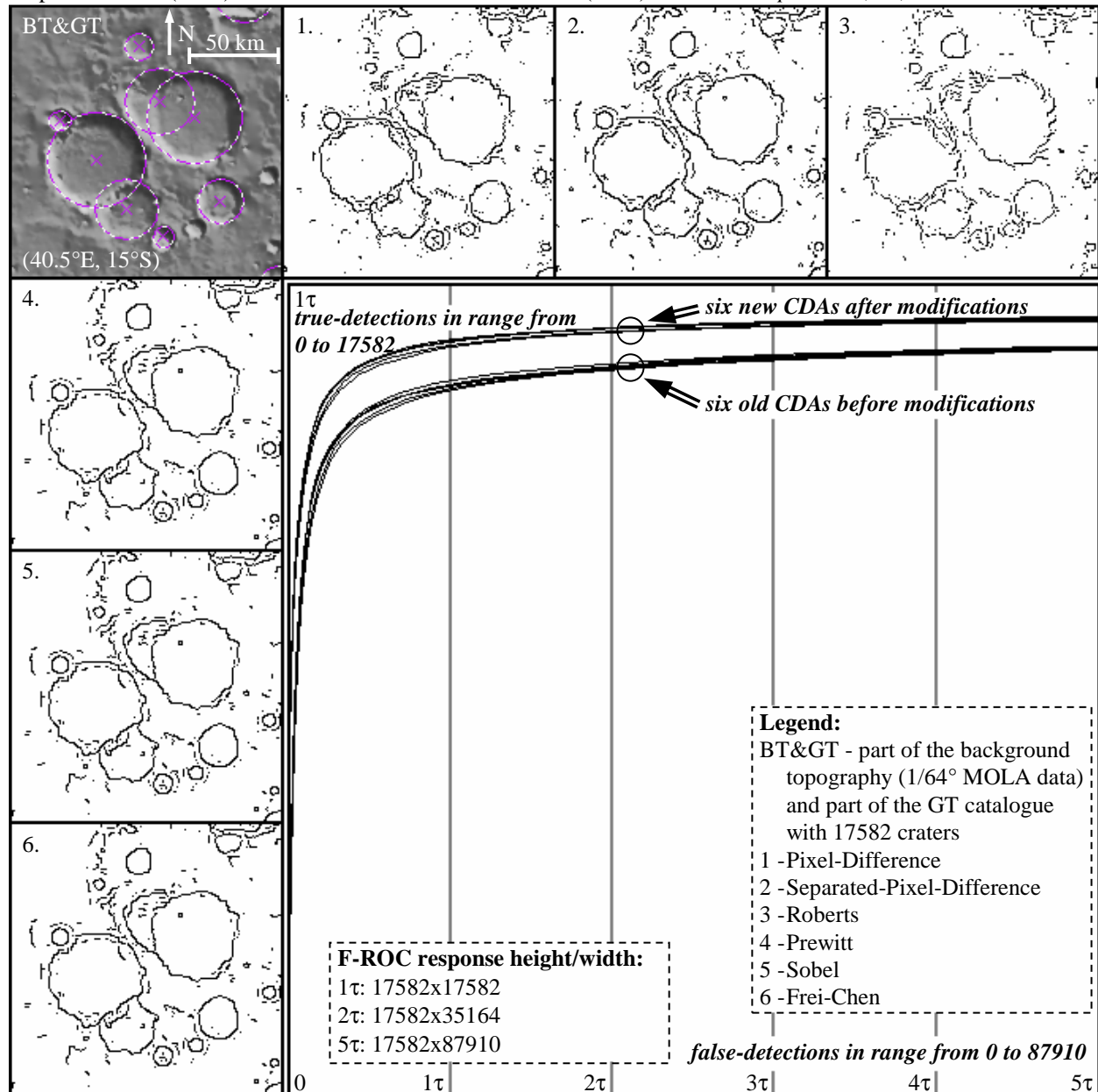


Figure 1: Detected edges (left and top) and F-ROC evaluations (right-bottom) for operators from Table 1.